COMPARISON OF TEMPERATURE DIFFERENCE MEASUREMENT TECHNOLOGIES USED IN VEHICULAR HEAT EXCHANGERS

Yuqi H.*, Xiaoli Y., Zhentao L., and Rui H.
*Author for correspondence
Power Machinery and Vehicular Engineering Institute,
Zhejiang University,
Hangzhou 310027,
P.R.China
Abbreviation E-mail: huangyuqi@zju.edu.cn

ABSTRACT

In the vehicle industry, thermal balance experiments are extensively conducted on engines to determine energy distribution from fuel to engine power. The temperature differences between the hot and cold sides of the vehicular heat exchanger are the key data used to calculate heat quantity. However, in certain gas–liquid heat exchangers, the temperature difference of the liquid side is significantly smaller than that of the gas side. Measuring error is increased when adopting an inappropriate measurement method. To minimize error, a temperature difference measurement method based on compound thermocouple (CTC) is introduced in this paper. This method is calibrated using a thermostatic oil tank. An empirical formula is used to calculate cases in which the basic temperature ranges from 20 ℃ to 120 ℃, and a temperature difference of less than 20 ℃isgained. The proposed method is applied in a practical thermal balance experiment using a vehicle radiator, and the results are compared with that obtained by measuring with pairing calibrated resistance temperature detectors. Results show that the CTC can reduce thermal balance error in vehicular cooling systems to less than 4%.

INTRODUCTION

Thermal balance experimentation is one of the most important means of studying energy distribution in engines[1]. The energy produced by combustion in the chamber is mainly distributed into engine power, cooling heat, and exhaust dissipation[2]. To calculate the heat dissipation from the cooling system, the temperature difference between the inlet and outlet must be measured. Temperature sensors are normally used to measure local temperatures, and temperature difference is calculated based on the measurements. However, in certain vehicular heat exchangers, such as lubricating oil coolers and water radiators, the temperature difference in the liquid side is obviously smaller than that in the airside. The measurement accuracy easily influences the tested difference value, thereby affecting the precision of the thermal balance of the engine[3]. Furthermore, as power density in engine development increases, the mass flow rate($\dot{m}$) of liquid coolant in the heat exchangers increases as well; the error in temperature differences (ΔT) is thus amplified when calculating heat dissipations ($\dot{Q}_c$) using $\dot{Q}_c = C_{pc}\dot{m}\Delta T$, where C_{pc} is the specific heat capacity of the coolant. Therefore, ensuring precise temperature difference measurement is the key factor in engine thermal equilibrium experiments.

Several techniques have recently been introduced to improve the precision of temperature difference measurement. The most common method is using a temperature difference transmitter. Pairing resistance temperature detectors (RTDs) by means of calibration is an alternative method of minimizing test error[4].

Temperature difference transmitters use hardware to process the temperature signal between two measuring points. Such transmitters consist of the gate circuit, holding circuit, and A/D circuit. The temperature difference signals are converted into analog signals during processing. The accuracy of this approach mainly depends on the temperature signals at the input terminal. This approach therefore has a considerably high requirement for temperature sensors. Furthermore, this method is based on the principle of signal transmission, which implies a certain amount of transmission error. Typically, when the accuracy of the temperature difference transmitter is approximately 1% F.S, the measurement error ranges from 0.5 ℃ to 2 ℃. However, in the field of vehicular heat exchangers, given conditions of relatively small temperature difference and high mass flow rates in the liquid side, the actual temperature difference between the import and export is less than 10 ℃. Therefore, measurement error significantly affects the calculation of thermal balance, the error oh which could exceed 5%.

The aim of pairing the RTDs by means of calibration is to minimize measurement error by identifying two temperature sensors with the same positive or negative error deviations. All temperature sensors are calibrated in the same batch. Particular sensors with the same shift direction and the closet calibration values are selected to form the pairing sensors used to measure the import and export

temperatures, respectively, of the same heat exchanger. In this method, the error resulting from opposite trends or inconsistency among the sensors can be minimized. However, the process of calibration and selection are too complicated to be widely used in the industry.

To ensure precision and to streamline the operation, a temperature difference measurement method based on compound thermocouple (CTC) is introduced in this paper. The principle of this method is stated, and the empirical formula used in practical applications is derived accordingly. The method is validated and compared with pairing RTDs by means of practical thermal balance experiments in a wind tunnel system. This method is more convenient and useful in measuring the temperature differences in vehicular heat exchangers.

PRINCIPLE OF THE MEASURING METHODS

The structure of the compound thermal couple is shown in Fig. 1. X_1 and X_2aretwo thermal couples composed of A_1 + B_1 and A_2 + B_2. A_1 andA_2aremade of the same material A, whereasB_1 andB_2aremade of the same material B. The B points of these two thermocouples are melted together (E_B represents the corresponding electric potential) to manufacture the CTC. In application, the sensors of X_1 and X_2arelocated at the required test points(T_1+ΔT and T_1represent the tested temperatures, ΔT>0). A_1 and A_2arethe measuring cables of the CTC(E_{A1} and E_{A2} represent their respective thermoelectric potentials). The three terminals A_1, A_2, and E_B are kept at the same environmental temperature T_0[5].

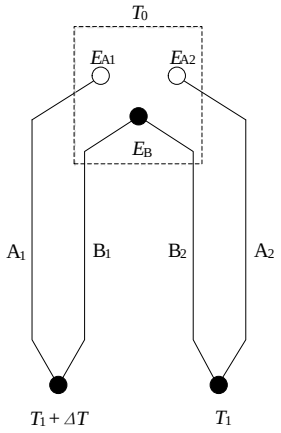

Figure 1 Principle of compound thermal couple

The thermoelectric potentials of the reference points in the compound thermal couple are:

$$E_{A_1A_2} = E_{A_1B} - E_{A_2B} \qquad (0)$$

At the same time,

$$E_{A_1B} = \int_{T_0}^{T_1+\Delta T} S_{AB}(T)\,dT \qquad (0)$$

$$E_{A_2B} = \int_{T_0}^{T_1} S_{AB}(T)\,dT \qquad (0)$$

where $S_{AB}(T)$ is the Seebeck coefficient[6]used to create the thermocouple using materials A and Band can be calculated using the following formula:

$$S_{AB}(T) = \int_0^T \frac{\mu_A(t)\cdot\mu_B(t)}{t}\,dt \qquad (0)$$

where μ is the Thomson coefficient obtained by especial experiment.

From the four equations above, the equation below is obtained:

$$E_{A_1A_2} = \int_{T_1}^{T_1+\Delta T} dT \int_0^T \frac{\mu_A(t)\cdot\mu_B(t)}{t}\,dt \quad (0)$$

where the Thomson coefficient μ is a constant and E_{A1A2}isthe function of T_1(basic temperature) and ΔT (temperature difference), which can be written as:

$$E_{A_1A_2} = f(T_1, \Delta T) \qquad (0)$$

CALIBRATION OF MEASURING SYSTEM

The calibration system (shown in Fig.2) consisted of two thermostatic fuel tanks, two T-type(Copper/copper-nickel alloy) thermocouples, two high-precision mercury thermometers, and one CTC. When calibration was performed, the steady temperature difference was adjusted using two thermostatic oil tanks. The instruments mentioned above and the sense points of the CTC were then placed in the fuel tank, as shown inFig.2.

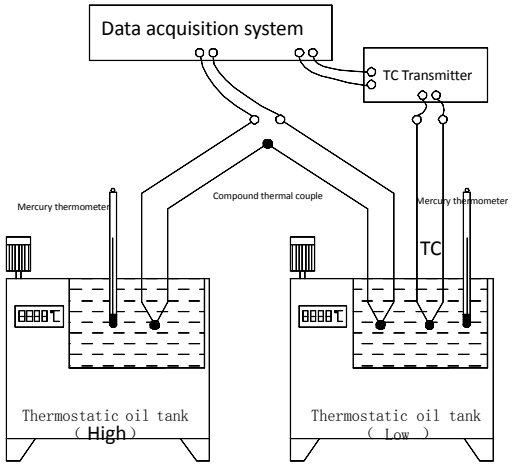

Figure 2 Schematic of calibration of sensors

During calibration, the lower temperature between the two oil tanks was taken as the basic temperature *T*, which was measured using a mercury thermometer. The basic temperature *T* was set to five levels in calibration: 60 ℃, 80 ℃, 100 ℃, 120 ℃,and 140 ℃.The temperature difference *ΔT* of two oil tanks variedfrom2 ℃to10 ℃perbasic temperature level. Calibration data was acquired using a data

acquisition system produced by National Instruments[7]. The TC signals used to measure the basic temperature were acquired using the thermocouple data acquisition module; the thermoelectric potential signals measured using the compound thermal couple were acquired using a micro-voltage data acquisition module. Synchronous acquisition was achieved by using a real-time controller in an industrial computer.

By collecting the temperature difference, electrical potential difference, and the basic temperature data obtained during calibration, the curves where the temperature difference thermoelectric power ΔE versus basic temperature T and temperature difference ΔT are plotted below.

As shown in Figs.3 and 4, the temperature difference thermoelectric power ΔE, the basic temperature T, and the temperature difference ΔT exhibit a significant positive correlation. Taking the temperature difference ΔT as the dependent variable, with the thermoelectric potential ΔE and the base temperature T as the independent variables, the results can be analyzed by using the binary linear and nonlinear regression methods, respectively.

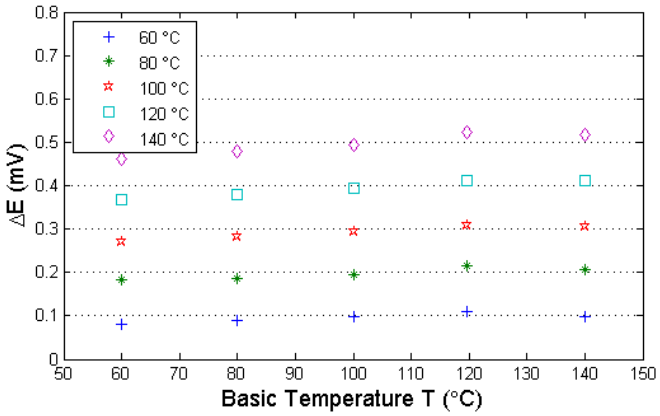

Fig.3 ΔE at various basic temperatures T

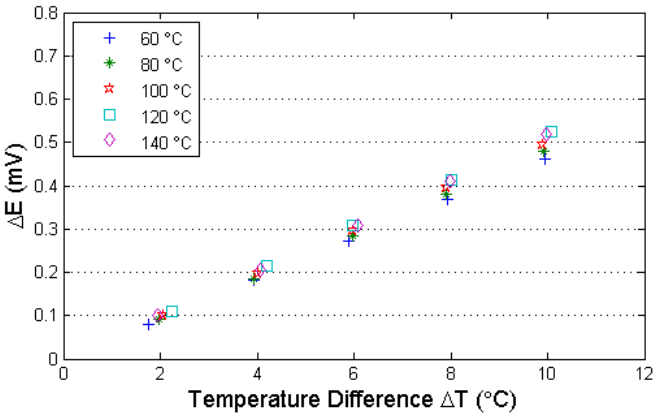

Fig.4 Δ E at various temperature differences ΔT

The result of the linear regression model is as follows:

$$\Delta T = a + bT + c\Delta E \qquad (0)$$

where a, b, c are the estimated parameters of this regression, and which can be calculated using the least squares method:

a=0.9213, b=-0.0081, c=19.9006

The result of the nonlinear regression model is described as follows:

$$\Delta T = a * T^{b} * \Delta E^{c} \qquad (0)$$

The parameters calculated using the least square method are as follows: a=36.356, b=-0.133, c=0.979.

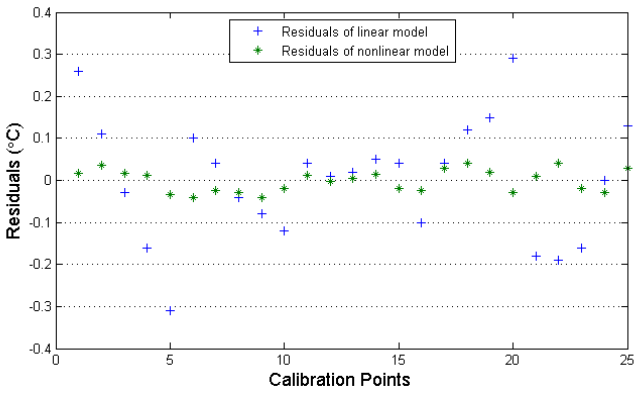

Fig.5 Residuals analysis results

Fig.5 shows the residual analysis results of the above models. The regression range of the linear model was found to be [-0.3, 0.3] ℃. By contrast, the regression range of the nonlinear model was [-0.04, 0.04] ℃, which is much more accurate than the former result. One possible reason for this result is shown in Equation(5):an obvious non-linear relationship exists between thermoelectric power E and temperature difference ΔT, and between thermoelectric power E and base temperature T. Therefore, the empirical formula is expressed as:

$$\Delta T = 36.356 * T^{(-0.133)} * \Delta E^{0.979} \qquad (0)$$

To analyze the relative error of the CTC empirical formula, the log of Equation(8)is taken on both sides:

$$\ln \Delta T = \ln a + b \ln T + c \ln(\Delta E) \qquad (0)$$

After the derivation,

$$\frac{d(\ln \Delta T)}{dT} = \frac{\delta(\Delta T)}{\Delta T} = \frac{a}{T} + c\frac{\delta(\Delta E)}{\Delta E} \quad (0)$$

The relative measuring error based on the empirical formula can thus be expressed as:

$$\left|\delta(\Delta T)\right| = \left|\frac{a}{T}\right| \cdot \left|\Delta T\right| + \left|c\frac{\delta(\Delta E)}{\Delta E}\right| \cdot \left|\Delta T\right| \quad (0)$$

The adopted the estimated parameters of the non-linear regression model are as follows: a=36.356, b=-0.133, and c=0.979.Assuming that basic temperature was 100 ℃ and the temperature difference thermoelectric power was 472mV (equal to the case where temperature difference is10 ℃), the relative deviation caused by the CTC was only 0.033 ℃, far less than that resulting from using an ordinary T-type thermocouple or two T-type thermocouples(about 0.2 ℃[8]).

Based on empirical Equation(9), as long as the radiator inlet temperature and the thermoelectric powers are measured, the temperature difference between the inlet and outlet can easily be calculated. The empirical formulas can be applied to all the results tested using CTCs consisting of A and B, with no need to calibrate one by one. This process is particularly well-suited for engine thermal balance experiments, which has several heat exchangers to be measured continuously at various working conditions.

According to the calibration, this empirical formula is appropriate for use in cases in which the basic temperature ranges from 20 ℃ to 120 ℃and the temperature difference is less than 20 ℃.

VALIDATION AND RESULT ANALYSIS

1. Test system and experimental scheme

To validate this CTC-based method, radiator thermal balance performance tests were conducted on a wind tunnel system. The tested radiator was a traditional compact heat exchanger which consisted of plate fins and a flat tube, and the structure parameters are listed in Table1.Water was used as the hot-side medium and air was used as the cooling medium. The hot-side temperature difference in the radiator was measured in two facilities simultaneously: pairing calibrated RTDs[4] and using a CTC. For the cold side, the temperature was measured using measuring nets with a standard uncertainty of ±0.5K fitted in the upstream and downstream of the radiator.

Table 1 Specification of the vehicular radiator

Parameter	Size
Length(mm)	820
Width(mm)	56
Height(mm)	644
Tube height(mm)	2
Fin height(mm)	7.5
Upwind area (m^2)	0.528
Heat transfer area z(m^2)	40.27

In actual application, the cold-side heat absorption was always less than the heat dissipation at the hot side because of the heat capacity of the heat exchanger. The closer these two results are to each other, the better the thermal balance is. Thus, our objective was to find better facilities with the smallest error and using a convenient operation.

Fig.6 displays the wind tunnel system for measuring the thermal balance in the radiator. The inflow water temperature was maintained at 85 ℃and the ambient temperature (the temperature of cold air) was approximately 32 ℃. The hot-side mass flow rate was set as 1.7, 3.4, 5.1, and 6.8kg/s. The air flow velocities were adjusted to 2, 5, 7, and10m/s.

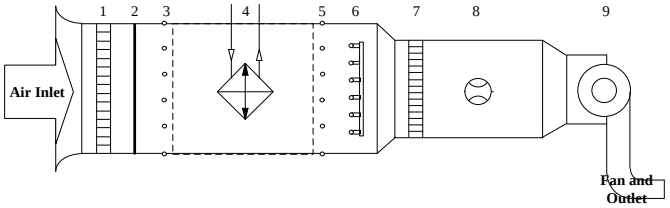

(1)Honeycomb straightener, (2) inlet air temperature mesh, (3) pressure tube (inlet), (4)Water radiator, (5) pressure tube (outlet), (6) outlet air temperature mesh; (7) honeycomb straightener, (8) airflow meter, and(9)exhaust fan and air outlet

Fig.6 Schematic of the thermal balance test system

Normally, water is an ideal fluid with constant density and specific heat capacity. However, the effect of temperature variation on the physical properties of water cannot be disregarded when calculating the heat exchange. Thus, the physical properties of water in the actual application were fitted with the regression equations used in IAPWS-IF97[9].

Density is calculated as:

$$\rho = V_i \cdot \mathrm{MoleWt} \quad \left(\mathrm{kg/m^3}\right),$$

$$V_i = \frac{A}{B^{\left(1+\left(1-\frac{T}{C}\right)^D\right)}} \quad \left(\mathrm{kmol/m^3}\right) \qquad (0)$$

A=4.6173, B=0.26214, C=647.29, D=0.23072.

where T denotes the thermodynamic temperature and MoleWt represents the molecular weight of water.

Specific heat capacity is given by:

$$C_p = \frac{C_{pL}}{\mathrm{MoleWt}} \quad \left(\mathrm{kJ/kg\cdot ℃}\right), \qquad (0)$$

$$C_{pL} = a + bT + cT^2 + dT^3 \quad \left(\mathrm{kJ/kmol\cdot ℃}\right)$$

a=4.6173, b=0.26214, c=647.29, d=0.23072.

The parameters of the hot side were selected as a reference value to evaluate the error of thermal balance performance test because the cold-side (air) temperature difference and velocity were larger than those of the hot side (water).The air velocity in the wind tunnel was significantly lower than the speed of sound; therefore, we considered the cooling air as an incompressible ideal gas[10] and the temperature as the only reason for the density variation. The air used in the actual experiments was moist air and the corresponding physical parameters were calculated using the following equations[11]:

Absolute humidity H is written as:

$$H = 0.662 \cdot \phi \cdot \frac{p_g}{p_0 - \phi \cdot p_g} \qquad (0)$$

where ϕ denotes relative humidity, p_g represents the saturated water vapor pressure, kPa; and p_0 denotes the standard atmospheric pressure.

According to Antoine equation[12],

$$\ln\left(p_g\right) = A - \frac{B}{T+C} \qquad (0)$$

Here, A, B, and C represent the Antoine constants: A=9.3876, B=3826.36, and C=-35.85. T ranges from 290Kto 500K.

Specific volume is calculated as:

$$v_H = \left(0.772 + 1.224H\right) \cdot \frac{\left(273 + t_n\right)}{273} \cdot \frac{p_0}{p_a} \qquad (0)$$

$$\left(\mathrm{m}^3/\mathrm{kg}\right)$$

t_n denotes the temperature at the measuring plane, ℃, and p_a are used to obtain the local atmospheric pressure, kPa.

Density[13] can be expressed as:

$$\rho = \frac{1}{v_H} \quad (kg/m^3) \qquad (0)$$

Specific heat capacity is given by:

$$C_p = 1.01 + 1.88H \quad \left(\mathrm{kJ/kg}\cdot℃\right) \qquad (0)$$

Based on these above equations, C_p and ρ only depend on absolute humidity H, temperature t_n , and atmospheric pressure p_a .

2. Validation of the method

The Effectiveness-*NTU* method (ε-*NTU*) was used to evaluate the test results. Based on the working condition of this vehicular radiator, the corresponding *NTU* number ranged from 0.5 to 1.8when it was operated on its characterized boundary condition. This radiator had across-flow pattern; therefore, the relationship of ε-*NTU* is defined using the following equation[14]:

$$\varepsilon = 1 - \exp\left(\frac{NTU^{0.22}}{C^*}\left[\exp\left(-C^* NTU^{0.78}\right) - 1\right]\right) \qquad (0)$$

$$\varepsilon = \dot{Q} \Big/ \dot{Q}_{\max}, \quad C^* = \frac{C_{\min}}{C_{\max}} \qquad (0)$$

In this equation, effectiveness $\varepsilon = \dot{Q} \Big/ \dot{Q}_{\max}$ represents the ratio of the actual heat transfer rate to the maximum possible heat transfer rate. $C^* = \frac{C_{\min}}{C_{\max}}$ denotes the heat capacity rate ratio. Heat transfer unit number $NTU = \frac{UA}{C_{\min}}$ stands for the dimensionless heat transfer scale of the radiator. The larger *NTU* is, the closer ε is to its theoretical limit.

The distribution of ε-NTU found in a previous study[15]and calculated using the test results of the CTC-based method are shown in Fig.7. The solid lines represent the empirical curves for this type of radiator, and the small circles show the calculated value resulting from the test of the CTC. As shown in Fig. 7, all of the working points measured by using the CTC are within the range of the empirical curves. This trend proves that the test results are reasonable and believable.

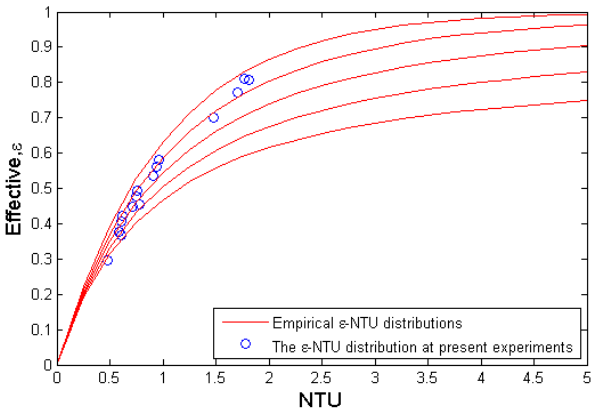

Fig.7 Distribution of ε-NTU of the radiator

3. Effect of velocity variation

Fig.8 plots the curves of the hot-side temperature difference with various water mass flow rates. The dashed line represents the value measured by pairing calibrated RTDs, and the solid lines represent the results of the CTC-based method.

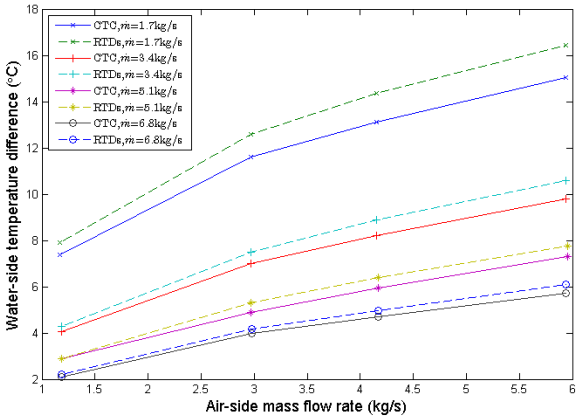

Fig.8 Water-side temperature difference

As shown by the curves, the results using the CTC-based method were less than those using the pairing of calibrated RTDs at all conditions. As the flow rate increased, the deviation between the pairing of calibrated RTDs and CTC-based method increased. This tendency might be

because for the test using the RTDs, when temperature was high, the deviation was larger[16].

All of the measured temperature differences increased as the air flow rate and water flow rate exhibited similar trends. Although the pairing of RTDs resulted in either negative deviations or positive deviations through calibration and selection, the measuring errors increased as the temperature difference increased, and accumulated in relation to the measured results throughout the test process. Thus, all of the temperature differences measured using RTDs were always larger than those measured using CTCs.

4. Effects of temperature difference on test precision

Figs.9 to 12 display the heat transfer versus cold-side velocity at different water flow rates. The quantities of heat transfer were calculated by using the hot-side results of pairing calibrated RTDs, the hot-side results of the CTC-based method, and the cold-side temperature differences (measured by using a temperature measuring net).

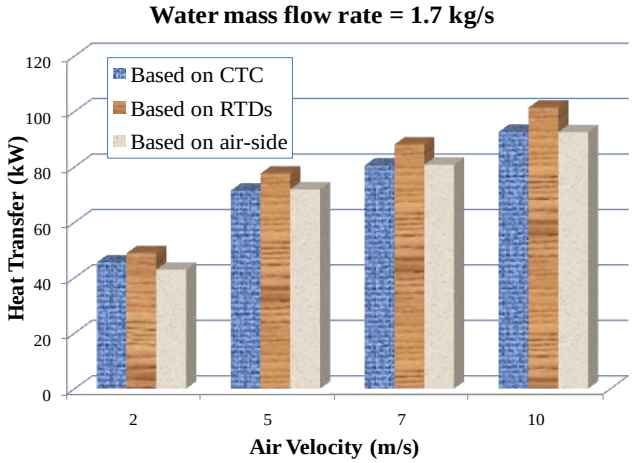

Fig.9 Comparison between measured heat transfer rates when the water-side mass flow rate is1.7kg/s

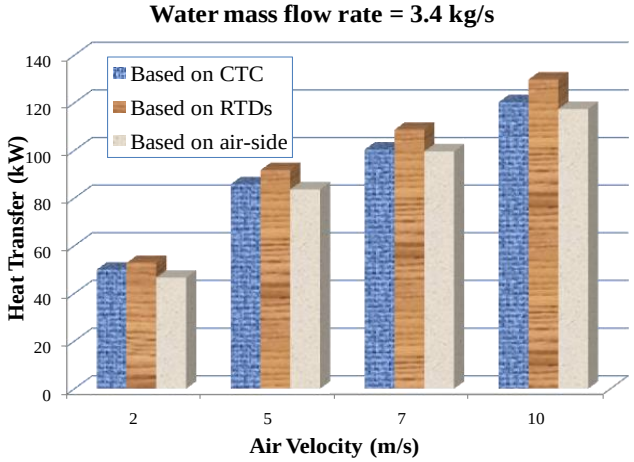

Fig.10 Comparison between measured heat transfer rates when the water-side mass flow rate is3.4kg/s

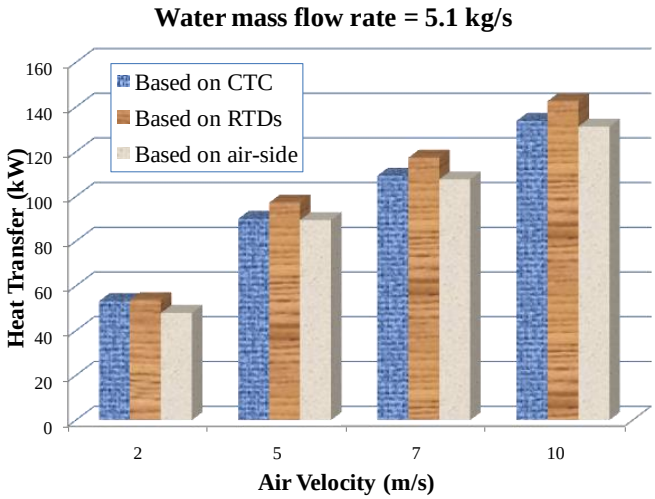

Fig.11 Comparison between measured heat transfer rates when the water-side mass flow rate is5.1kg/s

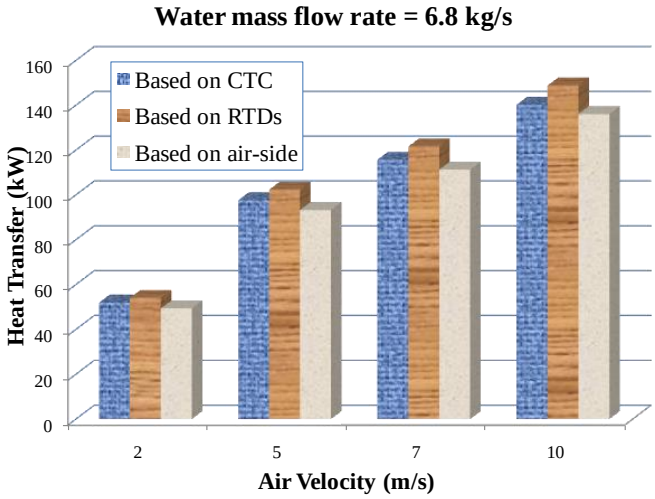

Fig.12 Comparison between measured heat transfer rates when the water-side mass flow rate is 6.8kg/s

Figs.9 to 12 show that $\dot{Q}_{air} < \dot{Q}_{TC} < \dot{Q}_{RTD}$. At all conditions, the heat dissipation calculated using the results of the CTC-based method was significantly closer to the cold-side heat absorption.

According to the error equation of thermal balance [17],

$$E = \frac{2(q_w - q_a)}{(q_w + q_a)} \times 100\% \qquad (0)$$

We calculated the thermal balance error using the results of pairing calibrated RTDs and CTC-based method, as shown in Fig.13. Here, the dotted line represents the thermal balance error calculated using the results of pairing calibrated RTDs, and the discrete points stand for the error using the CTC-based method.

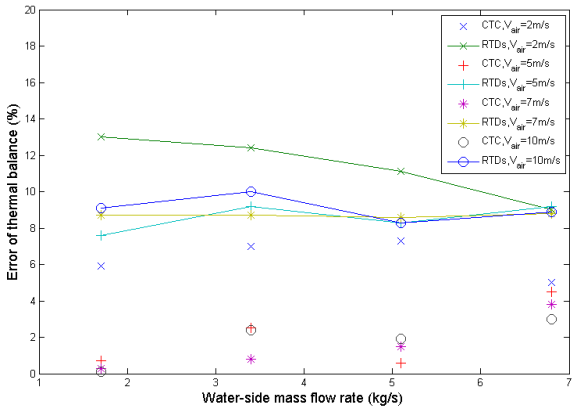

Fig.13 Error of the thermal balance tests

In Fig. 13, the averaged thermal balance error from pairing calibrated RTDs was approximately9.4%.When the air velocity was only 2m/s, the radiator was in the worst cooling condition, and the maximum error reached 12.4%. However, for the CTC-based method, the averaged error was only about 3.174%, and in most conditions, the error from CTC was less than 5%.These results indicate that the application of the CTC-method greatly improved the accuracy of the temperature difference measurements.

CONCLUSION

A temperature difference measurement approach based on CTC was proposed in this study. The principle of this method was extrapolated, the CTC was calibrated, and the approach was validated by conducting thermal balance experiments in a wind tunnel. The empirical equations suitable for cases where the basic temperature ranged from 20 ℃ to 120 ℃ and the temperature difference less than 20 ℃,werededuced according to calibration.

The test results indicate that in a vehicular heat exchanger with a large liquid-flow rate and small temperature difference, using the CTC-based method can greatly minimize the error of thermal balance. In conclusion, the CTC-based method is low cost, convenient, and accurate. Compared with the pairing calibration method, the averaged error of thermal balance can be reduced to less than 4% by applying the CTC-based method.

REFERENCES

[1] Michelle Tarquis Ngy-Srun Ap. Innovative Engine Cooling Systems Comparison[J]. SAE Paper, 2005, 2005-01-1378.
[2] X G. Wang Z P. Yao. Cooling and Heat Transfer of Vehicle[M]. Beijing: Beijing University of Technology Press, 2001, 96-148.
[3] F lv. The investigation on match and design of commercial vehicle cooling module[D]. Zhejiang: Zhengjiang University, 2011, 1-20.
[4] S.J.SONG T.KIM, T.J.LU. fluid-flow and heat-transfer measurement techniques[M]. 2009,
[5] S. Han. Fundamental Research on Intelligent Cooling System for Vehicle Engines[D]. Zhejiang: Zhengjiang University, 2012, 27-33.
[6] Safa Kasap. Thermoelectric effects in metals: thermocouples[J]. Canada: Department of Electrical Engineering University of Saskatchewan, 2001
[7] Jeffrey Travis, Jim Kring. LabVIEW for Everyone: Graphical Programming Made Easy and Fun (National Instruments Virtual Instrumentation Series)[M]. Prentice Hall PTR, 2006.
[8] Dong Junqi , Chen Jiangping , Chen Zhijiu. Heat transfer and pressure drop correlations for the wavy fin and flat tube heat exchangers[J]. Applied Thermal Engineering, 2007, 27(11): 2066-2073.
[9] Wolfgang Wagner , Alfred Kruse , Hans-Joachim Kurtzschmar. Properties of water and steam: the industrial standard IAPWS-IF97 for the thermodynamic properties and supplementary equations for other properties: tables based on these equations[M].Springer-Verlag Berlin, 1998.
[10] ANSYS FLUENT ANSYS. 12.0 User's Guide[M]. ANSYS Inc, 2009
[11] Yunus A Cengel , Michael A Boles , Mehmet Kanoğlu. Thermodynamics: an engineering approach[M]. Vol. 5McGraw-Hill New York, 2011.
[12] WOLFGANG WAGNER , JR Cooper , A Dittmann , etc. The IAPWS industrial formulation 1997 for the thermodynamic properties of water and steam[J]. Journal of Engineering for Gas Turbines and Power, 2000, 122(1): 150-182.
[13] T Fujii , Y Kato , K Mihara. Expressions of transport and thermodynamic properties of air, steam and water [J]. Sei San Ka Gaku Ken Kyu Jo, Report, 1977, (66)
[14] Chi-Chuan Wang , Ralph L Webb , Kuan-Yu Chi. Data reduction for air-side performance of fin-and-tube heat exchangers[J]. Experimental Thermal and Fluid Science, 2000, 21(4): 218-226.
[15] William Morrow Kays , Alexander Louis London. Compact heat exchangers[M]. 1984
[16] PRN Childs , JR Greenwood , CA Long. Review of temperature measurement[J]. Review of scientific instruments, 2000, 71(8): 2959-2978.
[17] ASHRAE Standard. 41.1 (1986) Standard method for temperature measurement[J]. American Society of Heating, Refrigerating, and Air-Conditioning Engineers, Inc., Atlanta, USA, 1986,